Effect of Humidity on Scintillation Performance in Na and Tl Activated CsI Crystals

Pin Yang, Charles D. Harmon, F. Patrick Doty, and James A. Ohlhausen

***Abstract*—Time dependent photoluminescence and radioluminescence for sodium (Na) and thallium (Tl) activated cesium iodide (CsI) single crystals exposed to 50% and 75% relative humidity (RH) has been investigated. These results indicate that Tl activated crystals are more robust than the Na activated crystals against humidity induced scintillation degradation. The development of "etching pits" and "inactive" domains are the characteristics of deteriorated Na activated CsI crystals. These "inactive" domains, bearing a resemblance to a polycrystalline appearance beneath the crystal surface, can be readily detected by a 250 nm light emitting diode. These features are commonly observed at the corners and deep scratched areas where moisture condensation is more likely to occur. Mechanisms contributing to the scintillation degradation in Na activated CsI crystals were investigated by Time-of-Flight Secondary Ion Mass Spectrometry (ToF-SIMS). ToF-SIMS depth profiles indicate that Na has been preferentially diffused out of CsI crystal, leaving the Na concentration in these "inactive" domains below its scintillation threshold.**

***Index Terms*—Cesium iodide, dopants, failure mechanisms, scintillation detectors.**

I. Introduction

SODIUM (Na) and thallium (Tl) activated CsI scintillators have been widely used for ionizing radiation detection since the late 1960's.[1] These detectors are comparable to the earlier discovered NaI(Tl) scintillator in terms of their energy resolution and proportionality.[2] These cubic alkali halide scintillators are relatively easy to grow, making them very cost effective in comparison to state-of-the-art non-cubic scintillators, such as $LaBr_3$ and SrI_2. Furthermore, these scintillators are rugged and less sensitive to temperature change and mechanical deformation. They are ideal candidates for field applications. Among these alkali halide scintillators, NaI(Tl) is most hygroscopic and will deteriorate due to water absorption if exposed to the atmosphere for any length of time. Therefore, NaI(Tl) must be encapsulated in an air-tight container for normal use. CsI crystals, on the other hand, are less hygroscopic and are expected to be more robust and flexible for detector design and integration.

In this paper, we focused on the time dependent scintillation performance of Na and Tl doped CsI detectors exposed to different relative humidity (RH) conditions (50% and 75% RH). It is well known that NaI(Tl) is quite sensitive to moisture.[3] The deterioration of its performance was first reported by Kerrigan [4] who discovered the development of an amorphous layer on the crystal surface and correlated its thickness to the counting efficiency of the detector. Vydai *et al.* [5][6] and Kudin [7], studied the scintillation characteristics of CsI(Tl) crystals and attributed the performance deterioration of these detectors to the penetration of quenching impurities at the surface layer due to damages induced in the grinding and polishing processes. Recent studies [8]–[10] on Na activated CsI detectors indicate the detection efficiency of these crystals degrade quite fast in a high humidity condition (80% RH). However, the same behavior was not observed in Tl doped CsI crystals.[10] Rosenberg [11] investigated Na diffusion in thermally evaporated CsI thick films ($40\ \mu$m) after aged at room temperature over a period of several days and observed ripening of NaI precipitates at the surface and depletion of these precipitates 20 um below the surface. He extrapolated his observations to the degradation of scintillation performance in CsI(Na) crystals. Based on these studies, it is clear that deterioration mechanisms in dissimilar scintillators can be quite different. All these studies referred to the development of a "dead" or "inactive" layer on the surface of deteriorated detectors were indirectly illustrated by the degradation in scintillation performance. The energy deposition processes in the CsI(Na) detector, including a "dead" layer, have been experimentally demonstrated by direct observation of an additional X-ray decay peak isolated from the main ^{57}Co photopeak that is supported by Monte Carlo simulation.[9] Readers who are interested in simulation results should refer to the original paper and references therein. These studies emphasize on the radioluminescence responses, but do not elucidate what is the "dead" layer, how the "dead" layer is developed, to what extend the "dead" layer can grow into the bulk crystal, and why the "dead" layer affects scintillation performance. These are the subject of this investigation. This study focuses on material interactions with moisture and provide a quantitative analysis to support our proposed degradation mechanism in CsI(Na) scintillators.

II. Experimental Procedure

Na and Tl activated CsI single crystals (PhotoPeak Inc., Chagrin, OH) were sliced into ~ 3 mm thin sections by a diamond coated wire saw. These thin crystals, with a cross-section area of

Manuscript received June 23, 2013; revised October 03, 2013; accepted December 04, 2013. Date of publication March 14, 2014; date of current version April 10, 2014. Sandia National Laboratories is a multi-program laboratory managed and operated by Sandia Operation, a wholly owned subsidiary of Lockheed Martin Corporation, for the U.S. Department of Energy's National Nuclear Security Administration under contract DE-AC04-94AL85000 .

P. Yang, C. D. Harmon, and J. A. Ohlhausen are with Sandia National Laboratories, Albuquerque, NM 87185-0958, USA (e-mail: pyang@sandia.gov).

F. Patrick Doty is with Sandia National Laboratories, Livermore, CA 94551-9402 USA.

Color versions of one or more of the figures in this paper are available online at http://ieeexplore.ieee.org.

Digital Object Identifier 10.1109/TNS.2014.2300471

2.3 cm X 2.3 cm, were subsequently lapped with 600 and 1200 grit silicon carbide sand papers and polished to 1 micron finish. These samples were divided into 3 groups to study the effect of humidity on scintillation performance. Each group consisted of one Na and one Tl activated CsI crystal. A pair of these samples were set aside and kept in an argon filled glovebox with moisture content below 0.2 ppm as a reference. The remaining samples were placed in an environmental controlled test chamber at room temperature under 50% and 75% relative humidity (RH) conditions for various times. After exposure in the controlled humidity environment for a designated time, these samples were briefly taken out to ambient condition (< 3 hours) for photoluminescence and radioluminescence measurements.

The photo-excitation and emission spectra of the Na and the Tl activated CsI samples were measured by a fluorometer (QuantaMaster, Photonic Technology International, Birmingham, NJ), using a Xe arc lamp as the light source. The fluorometer is equipped with a double monochromator on the excitation side and a single monochromator on the emission side. Photoluminescence responses were collected at 0.1 second and 0.25 nm per step. The energy spectra were measured at room temperature in a closed ("Dark") box by placing a sample directly on top of a photomultiplier tube (PMT, Hamamatsu R1924A). The PMT was positively biased at 1150 V (Ortec 660, Oak Ridge, TN). Optical grease was not used between the crystal and PMT so moisture can be in contact with these crystals again under controlled humidity conditions after photo- and radio-luminescence measurements. The pulse height spectrum was measured under 59.5 keV γ-ray excitation from a $^{241}\mathrm{Am}$ (9.72 μCi) source placed at a fixed distance ($\sim$ 12 cm). Signal from the PMT was pre-amplified (Canberra 2007B, Meriden, CT) and shaping amplified (Ortec 572), before sending into a multichannel buffer (Ortec 926). Pulse height spectrum was collected for 300 seconds and analyzed using Maestro (Ortec) multichannel analyzer (MCA) software. Specific amplification and pulse shaping time parameters for these samples were set at

1) CsI(Na) -20 X, 1 μsec shaping time, low level discriminator set at 91 mV,
2) CsI(Tl) -20 X, 3 μsec shaping time, low level discriminator set at 39 mV.

Under these conditions, the pulse height shows a 3.4% variation in a single measurement; however, day-to-day operations can vary up to 10%. The relatively large variations can be attributed to a poor optical coupling between crystal and PMT due to the absence of optical grease.

III. Results and Discussion

A. Optical Spectroscopy

The optical excitation (blue lines) and emission (red lines) spectra of the reference Na and Tl activated CsI crystals are given in Fig. 1. A 295 nm and a 370 nm long pass filters are used in the emission spectra collection for CsI(Na) and CsI(Tl) crystals to prevent artifacts due to a second order diffraction grating effect from the monochromater mirrors. These emission spectra have been compensated and corrected by the spectral quantum efficiency of the photomultiplier tube used in the fluorometer. Fig. 1 shows that the excitation and emission spectra peaked at

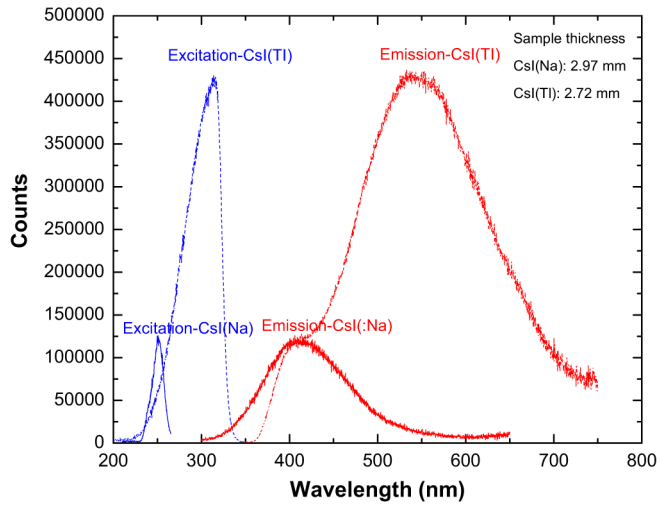

Fig. 1. The excitation (blue) and emission (red) spectra for the Na (solid line) and the Tl (dash line) activated CsI crystals.

250 nm and 407 nm for the CsI(Na) crystal (solid lines), and 317 nm and 540 nm for the CsI(Tl) crystal (dotted lines). The results clearly indicate that Na and Tl are both efficient activators with large Stokes shifts that can effectively reduce the amount of self-absorption and produce a high light yield. The source of the 250 nm excitation band in the CsI(Na) crystal is not clear, and the 407 nm emission band is related to the recombination of a self-trapped exciton immediately adjacent to the substitutional Na activator.[12]–[14] These self-trapped excitons have a strong electron-phonon coupling and will give a broad band emission.[15] The skewed broad excitation band peaked at 317 nm for the Tl^{+} activated CsI sample closely resembles six UV absorption bands (228 nm–290 nm) observed at liquid helium temperature.[16] The 540 nm emission for the CsI(Tl) sample was studied intensively for a long time. However, the nature of this emission is still under debate. The observation was interpreted as being a Tl^{+} intracenter transition [16], as dimer centers in CsI lattice [17], as a donor-acceptor recombination between a Tl^{0} and V_{k} centers [11], a recombination luminescence of an exciton captured at a Tl^{+} ion [18], and also as to the Jahn-Teller effect of two $^{3}\mathrm{P}_{1}$ sublevels of Tl^{+} ion [19]. All these mechanisms involve strong electron-phonon coupling that can lead to a broad emission band. Despite its thinner thickness, the Tl activated CsI (2.72 mm) exhibits a better light yield and a broader emission than the CsI(Na) sample (2.97 mm). It is believed that the combination of a large free gap below the 6p emitting level and a highly efficient $^{3}\mathrm{P}_{1}$ to $^{1}\mathrm{S}_{0}$ transition of the Tl^{+} (mercury-like) [20] ion gives a higher light output than the CsI(Na) sample, which is consistent with the relative absolute light yield reported in the literature.[21]

B. Radioluminescence Responses

In this study, a 60 keV gamma source ($^{241}\mathrm{Am}$) is used as our ionization radiation source to monitor the changes in pulse height spectra before and after samples are exposed to different humidity conditions for various amounts of time. The use of a weak gamma source helps to assess the vulnerability of the CsI

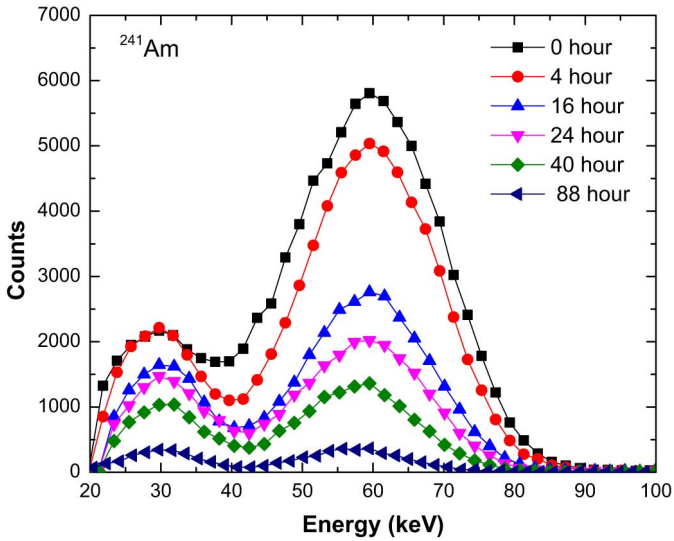

Fig. 2. The changes of pulse height spectrum as a function of time for CsI(Na) sample exposed to 75% relative humidity. An $^{241}\mathrm{Am}$ is used as an ionization source.

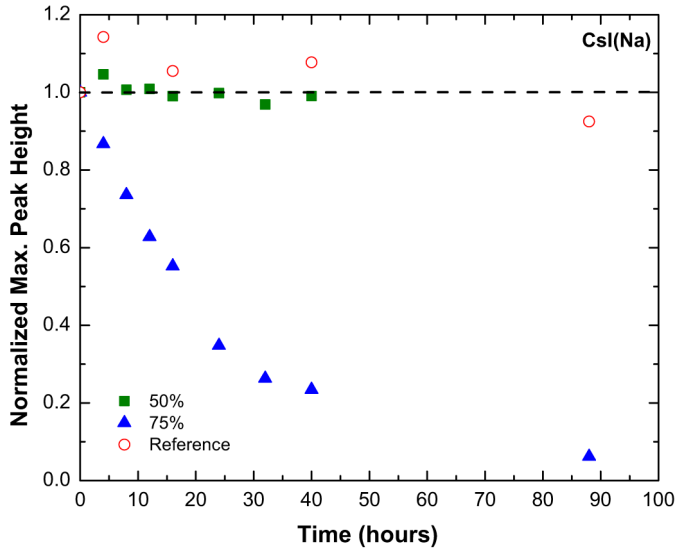

Fig. 3. The changes of the pulse height as a function of humidity and time for CsI(Na) crystals at room temperature.

detector with respect to the change of its scintillation properties due to the humidity effect.

Fig. 2 illustrates the evolution of the pulse height spectra excited by an $^{241}\mathrm{Am}$ source at room temperature for the Na activated CsI sample exposed to 75% humidity for various amounts of time. The results show that there are two bands peaked at 60 keV and $\sim$ 30 keV for each testing condition. The first spectrum peaked at 60 keV corresponds to the $^{241}\mathrm{Am}$ photopeak (or full energy peak) where all of the gamma-ray energy is converted to the electron kinetic energy by the photoelectron absorption process. The second spectrum peaked near 30 keV is attributed to three sources. One of these sources is the escape X-rays which usually happen near a surface of the detector, particularly for samples of thin geometry and the incident gamma ray energy is low and close to the -binding energy of K shell electrons of the absorber atoms in the detector material. Because CsI detector is in use and the binding energies of K_α for Cs and I are at 30.635 keV and 28.317 keV, the gamma rays that produce these escape X-rays can only deposit an energy equal to the original incident gamma-ray energy (60 keV) minus the bindingenergy of the K shell electrons ($\sim$ 30 keV) of the absorber atoms in the detector. This leads to an X-ray escape peak located at $\sim$ 30 keV. The second source contributing to this peak comes from the decay X-rays where a high energy electron falls back to K shell after a photoelectron is created by the incident gamma ray. These events are normally included in the full energy photopeak. on the pulse height spectrum. If some regions in the crystal become "inactive" (as it will be demonstrated in the later sections) ionized electrons generated in the absorption process can no longer produce photons. However, decay X-rays generated in this process can still ionize electrons in the adjacent "active" region and register its energy on the pulse height spectrum The observation of such an event is unique and can be used to identify the development of an "inactive" region in the CsI crystal when a higher energy gamma source such as a $^{57}\mathrm{Co}$ is used.[9] However, this process is limited to regions near the active-inactive interface because decay X-rays created in the "inactive" volume can be easily re-absorbed. For the CsI detector used in this study, the characteristic X-rays for both Cs and I are close to 30 keV; therefore, the decay X-rays from these absorber atoms can also contribute to the peak at 30 keV. The third source comes from a weak 26.24 keV emission (2.3%) from $^{241}\mathrm{Am}$.. Because the number of events due to escape X-rays and decay X-rays and 26.24 keV gamma rays are much smaller in comparison to the photons generated by the 60 keV gamma rays in the bulk CsI crystal, the photopeak observed in the pulse height spectrum is much greater than the small peak observed at 30 keV. Fig. 2 shows that the area under both these peaks decreases as the exposure time at 75% RH increases. The decrease of the total photon count for the photopeak indicates that the performance of the CsI scintillator has degraded as the total "active region" in the crystal decreases. The reduction of the pulse height (or total photons) for the photopeak also changes the relative peak height between the 60 keV and 30 keV peaks. When the scintillation performance of the crystal is almost completely diminished, the relative photon counts between photopeak and 30 keV peak changed from 0.28 to 0.68, which can be used as a signature for the degradation of the CsI(Na) crystals.

The normalized maximum pulse height at $^{241}\mathrm{Am}$ photopeak of these samples after being exposed to different relative humidity at room temperature for the CsI(Na) and the CsI(Tl) crystals are given in Fig. 3 and Fig. 4, respectively. For each measurement, the maximum pulse height (counts) for the photopeak was recorded and normalized to the initial reading to evaluate the changes induced by exposure to a humid environment at room temperature. Both figures show that the scintillation performance of the Na and the Tl activated reference samples and the samples exposed to 50% RH do not show significant change after 40 hours. However, the normalized maximum pulse height is significantly reduced for the CsI(Na) sample exposed to 75% RH (Fig. 3) where the counting efficiency reduces to 23.5% of

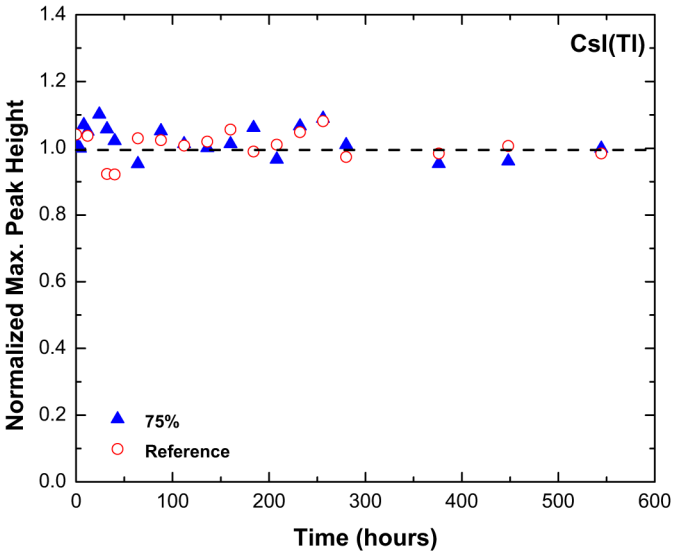

Fig. 4. The peak height as function of humidity and time for the CsI(Tl) crystals at the room temperature.

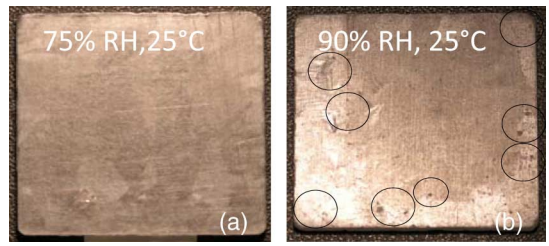

Fig. 5. The development of "domain" and "pitted" regions on the surface of CsI(Na) samples (2.3 cm X 2.3 cm) at room temperature. The change of appearance from single crystal to multi-domain and the development of pitted regions (dark spots as highlighted by circles) are shown for samples at (a) 75% RH and (b) 90% RH.

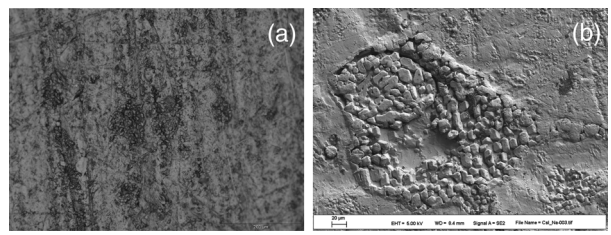

Fig. 6. Microphotographs of (a) optical image of the pitted regions on the surface of a CsI(Na) crystal after exposed to 90% RH for 49 hours, (b) SEM image of these pitted regions (scale $\mathrm{bar} = 20\ \mu\mathrm{m}$). These regions develop at scratches and edges of the sample.

their original values within the first 40 hours. Extending the exposure to a total of 88 hours, the normalized maximum peak height reduces to 6.2%, indicating that the ability of this sample to respond to ionization radiation from the $^{241}\mathrm{Am}$ source is almost completely diminished.

In contrast, the light output for the Tl activated CsI samples does not vary significantly over the first 40 hours. The variation of the data seems to be slightly larger than the day-to day change measured by our setup (10%) at the beginning. These variations can be attributed to the residual moisture on the crystal samples. By simply allowing the samples to air dry prior to taking a measurement, pulse height variations in the later measurements were reduced to pre-exposure levels. The results show that after extended exposure in a 75% RH up to 592 hours the test sample still tracks well with the reference sample and has not shown any sign of degradation in its scintillation performance. The robustness of the Tl activated CsI crystal is further demonstrated by a prolonged exposure of a CsI(Tl) sample in 75% RH at an elevated temperature of $60^{\circ}\mathrm{C}$ up to 216 hours (not shown). These observations are consistent with previous studies i.e., CsI(Tl) detectors will not suffer from scintillation deterioration if surfaces of these crystals are free from mechanical damages.[5]–[10].

C. Material Characterization

Initial inspection of these single crystal samples indicates that there are no special features on the surfaces except a few scratch lines induced during the grinding and polishing procedure. However, "domains" and "pitted" regions (dark spots) become visually noticeable (Fig. 5) on the surface of CsI(Na) samples after being exposed to 75% and 90% relative humidity for 40 hours. These "domains" give these crystals a polycrystalline appearance and can be easily identified by visual inspection. These regions tend to develop at the sample edges and deep scratch lines on the surface. Once developed, these features become more obvious as the exposure time increases. Particularly for the "pitted" regions, their size and number increased with additional exposure.

Fig. 6 shows an optical microphotograph and a Scanning Electron Microscopy (SEM) image of one of these "pitted" regions on the sample surface which has been exposed to 90% RH after 40 hours. The optical image shows these dark "pitted' regions (Fig. 6(a)). Their appearance looks like nodules or aggregates of small crystallites. The SEM image (Fig. 6(b)) shows these regions consist of clusters of small crystals recrystallized on the surface. Most of these small crystallites exhibit a hexagonal symmetry, suggesting the possibility of epitaxial recrystallization of the (111) plane from the CsI surface. The X-ray Energy Dispersed Spectroscopy (EDS) is unable to discern chemical differences between these regions and the bulk crystal, presumably the difference in chemical composition between these regions is below the detection limit of the EDS ($\sim$ 0.1 wt.%). This unique feature suggests that these regions might be developed as a result of localized moisture condensation and re-crystallization during the drying cycle. Therefore, it is conceivable that localized condensation at the CsI(Na) surface has dramatically decreases when relative humidity in the testing camber is controlled below (or equal to) 50%, resulting in no changes in its detector efficiency.

These surface features can also be observed on the surface of the CsI(Tl) sample ($60^{\circ}\mathrm{C}$, 75% RH for 24 hours) as illustrated in Fig. 7(a) and (b). These microphotographs are particularly interesting as they show that these small crystallites are preferentially nucleated and recrystallized at the deep scratches or edge areas where moisture can be easily condensed. However, the radioluminescence response of these CsI(Tl) samples does not change significantly. Continued exposure of this sample under the same condition (i.e., 75% RH $60^{\circ}\mathrm{C}$) does not enlarge these

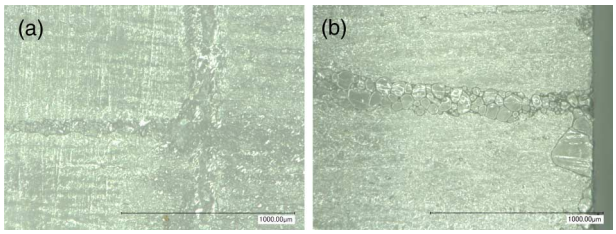

Fig. 7. The development of small crystallites due to the condensation of moisture on the scratched lines and the edge of a CsI(Tl) crystal (scale $\mathrm{bar} = 1$ mm).

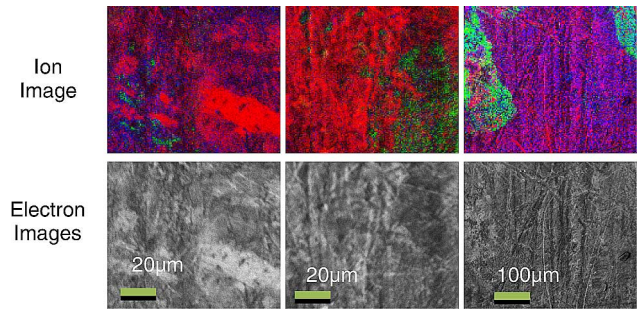

Fig. 8. The ToF-SIMS secondary ion images (top) and secondary electron images (bottom) taken from three different areas on a CsI(Na) sample that has been exposed to 75% RH for 88 hours. Images show the chemical distribution of CsI (red), Na and K (blue), and Na oxide/hydroxide (green) near these recrystallized areas.

regions or exacerbate its scintillation performance as demonstrated in Fig. 4.

A Time-of-Flight Secondary Ion Mass Spectrometers (ToF-SIMS, Model ION-TOF ToF.SIMS.5, Munster, Germany) is used to further investigate these recrystallization regions because this technique is particularly sensitive to the alkali elements (such as Na and K ions) due to their low ionization potentials. The technique sputters the study surface with a focused pulsed Bi^{3+} primary ion beam and collects and analyzes the ejected secondary ions by time-of-flight mass spectrometry. In the ToF-SIMS imaging mode, the primary ion beam is rastered across the sample surface similar to an electron microscopy while secondary mass spectra are recorded. This technique can give a submicron lateral resolution analysis of the chemical species on the surface while removing less than a monolayer of material from the surface. Additionally, secondary electrons generated by ion bombardment can be collected to generate secondary electron images in the ToF-SIMS system. In the ToF-SIMS depth profiling mode, positive 2 kVCs^{+} beam is used to remove material and the Bi^{3+} beam was employed for mass spectroscopy. By alternating these two ion beams, mass spectra can be collected as a function of depth from the surface, thus creating a depth profile.

Imaging data were acquired in a way that provided full mass spectra at every pixel in each image. These so-called spectrum images were processed using multivariate analysis methods described elsewhere.[22]–[24] The results from multivariate analysis are in the form of components, each of which have image (location and concentration) and spectra (identification) parts. From these components, a detailed qualitative analysis from the entire acquired spectrum is obtained.

Fig. 8 shows the ToF mass spectrometry multivariate results images (top) and the SEM images form the same region (bottom) of three areas with deep scratches and clusters of small crystallites, where red, blue and green represent the background CsI, the Na and K, and Na oxide/hydroxide, respectively. By referencing these color coded overlay images, it is obvious that the surface of these recrystallized regions are rich in Na (green) in comparison to their neighbor background (CsI–red). In contrast, the ToF-SIMS images of the reference sample only show the CsI background across the imaged areas.

Fig. 9, the -green component from Fig. 8, consists of three mass spectroscopy images and a mass spectrum from these recrystallized regions. The concentration of this spectral signature for these areas has been color coded, which increases as the color changes from black to bright yellow (as indicated on the right). Areas that have a higher concentration of this signature show an orange-red color on these images. The chemical identification of the recrystallized regions is given by the mass spectrum at the bottom of Fig 9, which is a histogram presentation of the distribution of secondary ions by the mass-to-charge ratio $(\mathrm{m/z})$. Based on the mass spectrum, the majority of the secondary ion fragments in these regions are Na^{+} $(\mathrm{m/z} = 23)$ and $\mathrm{Na_2OH}^{+}$ $(\mathrm{m/z} = 63)$. A small amount of Cs^{+} $(\mathrm{m/z} = 133)$ has also been detected. These Cs signals might be induced by the sputtering process from areas close to the bulk crystal, but can also be inadvertently deposited in the ToF-SIMS vacuum system as Cs is present as a volatile contaminant.

These results suggest that sodium has preferentially diffused out and accumulated on the surfaces sometimes in the form of an oxide, leaving behind "inactive" regions below the surface of the CsI crystal. The sodium concentration in these "inactive" regions must be below a concentration threshold where CsI can be an efficient scintillator. To verify the assumption, we compare the Na concentration depth profiles between the reference material and the sample exposed to 75% RH for 88 hours using ToF-SIMS depth profiles. Fig. 10 depicts the concentration profile of Na from crystal surface to the bulk in these samples. Data are reported by normalizing the Na ion intensity (counts per second) with the bulk signal from CsI based on the $\mathrm{Cs_2I}^{+}$ ion fragmentation. This procedure helps to minimize sample-to-sample and day-to-day variations in these measurements. Furthermore, the normalization will provide a more reliable comparison for the Na depth profiles without an elaborate calibration for the SIMS response (i.e., the relative sensitivity factor). Two regions from the sample exposed to 75% RH were measured (the red and blue depth profiles) for assurance. The results show that the Na concentration in these regions exhibits a greater exponential decay than the reference material (black) from the surface to the bulk CsI crystal. These data indicate that the sodium concentration for sample exposed to 75% RH drops almost 5 magnitudes from surface to ~ 3 μm deep and begins to level off at 0.0001 $(\mathrm{Na/Cs_2I}^{+})$. In comparison, the Na concentration decreases about 1 order of magnitude from surface to bulk (~ 1.5 μm) in the reference material. These results confirm that Na activators tend to preferentially diffuse outward to the surface of CsI crystals. Note the differences in Na concentration in the bulk of CsI crystals where Na in the reference material is at least one magnitude higher than the sample exposed to 75%

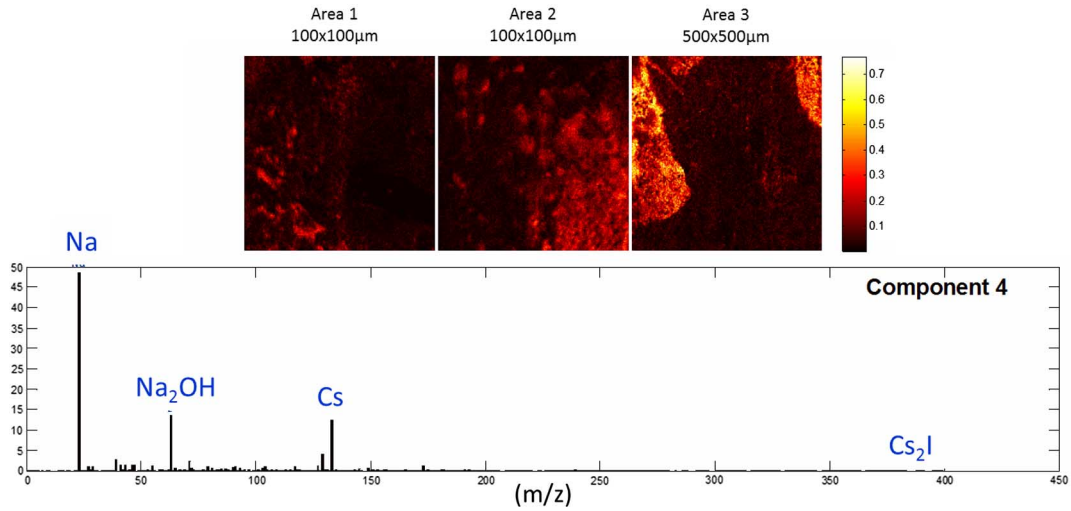

Fig. 9. SIMS images (top) and the chemical analysis (mass spectroscopy, bottom) showing the Na distribution on the sample surface and the recrystallized areas. The recrystallized areas show a higher Na concentration on the surface (more yellow).

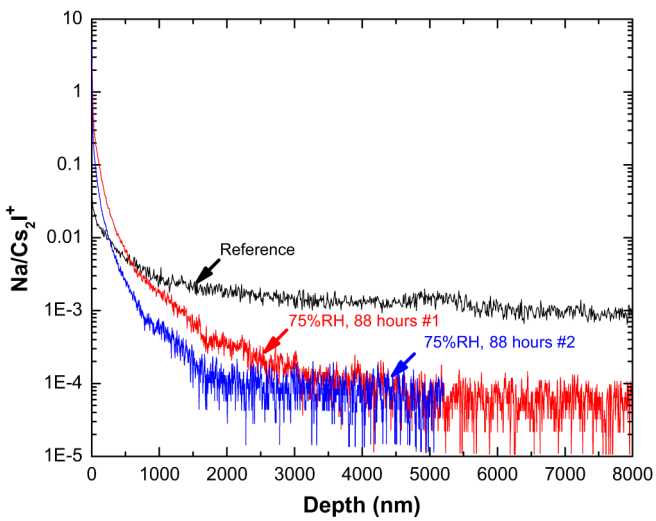

Fig. 10. A comparison of the Na depth profiles by ToF-SIMS depth profile analysis. The blue trace represents the Na concentration profile for the reference material while the red and green traces are for two different Na-rich locations on the CsI(Na) sample exposed to 75% RH for 88 hours.

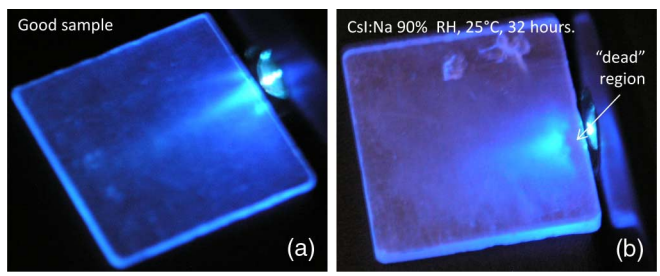

Fig. 11. The inspection of the "active" and "dead or inactive" regions in the CsI(Na) with a 255 nm LED.

RH. A typical Na doping concentration in the CsI scintillator is between 0.01 at.% to 0.04 at.%.[25] Assuming the Na concentration in our reference crystal is within this range, one will expect that "inactive" regions will be developed beneath the surfaces when Na ions diffuse out and its concentration is reduced one magnitude lower in the bulk crystal after sample exposed to 75% RH for 88 hours.

Based on the optical spectroscopy results (Fig. 1), one can easily inspect and identify the "active" and the "inactive" regions in a Na activated CsI crystal, using a light emitting diode (LED) whose emission matches the excitation peak of the CsI (Na) (i.e., 250 nm). Fig. 11 demonstrates the use of a LED in identifying the "active" and "inactive" regions in CsI(Na) samples. Fig. 11(a) shows a good sample where the entire crystal is active. It is shown that the region under 250 nm excitation has all been lightened up by its emission spectrum. In contrast, light emitted by the LED will be transparent to the "inactive" region and pass through without giving off any photoemission. Fig. 11(b) illustrates such a behavior, where 250 nm light from LED first passes through an "inactive" region and continues penetrating into the "active" region and creates a gap ($\sim$ 1 to 2 mm) between the LED and the "active" crystal. These "inactive" regions can have different sizes and geometries as they are initiated by localized condensation on the surface at different time. We have observed these "inactive" regions extend more than 1 cm into our large detector crystals. Therefore, the development of a "dead" layer should not be confined to a surface phenomenon. Although this technique does not provide any quantitative information, it is a practical method to screen and inspect crystals, particular when "inactive" regions have developed in CsI(Na) crystals. The lack of photoemission in these "inactive" regions and the discovery of Na rich regions on the surface of CsI crystal immediately indicate that Na in these "inactive" regions has diffused out of the crystal and left behind these regions with an activator (Na) concentration below the lowest limit for scintillation (i.e. 0.01%).[25]

There is further evidence to support the out-diffusion of sodium from the bulk CsI crystals. First, Na activated CsI crystals are more hygroscopic than Tl activated CsI crystals. The solubility of CsI in water is much less than NaI and TlI is insoluble in water at the ambient temperature (i.e., NaI: 184 grams, CsI: 44 grams, and TlI is insoluble in 100 cc of

water).[26] This could be attributed to a greater ionic nature between Na^+ and I^- (electronegativity difference $= 1.73$) than that between Tl^+ and I^- (electronegativity difference $= 0.64$) Generally, ionic compounds are more readily dissolved in a polar solution (such as water) than covalent compounds. Therefore, any localized surface condensation will impart a favorable condition to dissolve Na at the crystal surface and provide a driving force for Na to diffuse out. Second, the ionic radius of sodium is smaller (1.02 A) in comparison to the Tl (1.50 A) and Cs (1.67 A), and Na^+ ($m = 22.99$) is much lighter than Cs^+ ($m = 132.91$) and Tl^+ ($m = 204.37$); therefore, Na is more favorable than Tl to diffuse in the CsI lattice (lattice constant, $a = 4.567$ A). Furthermore, the greater covalent nature of the Tl-I bond will also increase the activation energy for Tl to diffuse in the CsI lattice. These arguments are consistent with the published data [27] where Na has the highest diffusion coefficient (D_o, diffusion coefficient at infinite temperature or pre-exponential diffusion coefficient) and the lowest activation energy in comparison to Cs, Rb and K in CsI crystals. Furthermore, the ripening process observed in the CsI thick films [11] demonstrates that Na can be quite mobile in the CsI lattice at room temperature. Therefore, CsI(Na) detectors must be encapsulated to prevent humidity induced deterioration. By the same token, the insolubility of TlI in water and the covalent nature between Tl^+ and I^- prohibit any interactions between moisture and CsI(Tl); therefore, scintillation deterioration is generally caused by an extrinsic factor such as the penetration of quenching impurities on mechanically damaged surfaces. [5]–[7] Although these arguments are suggestive, they seem to be consistent with microstructure study and surface chemical analysis.

IV. Conclusions

The effects of humidity on scintillation performance in Na and Tl activated CsI single crystals have been studied. The results show that the counting efficiency for the Na activated CsI crystals is more sensitive to ambient moisture than the Tl activated samples, as Na activated crystals are more hygroscopic than Tl activated crystals. Their scintillation performance decreases monotonically with the exposure time, particularly in higher humidity conditions (i.e., $RH > 50\%$). Therefore, special attention is required for storage and packaging these crystals for detector applications. Thallium activated CsI crystals have shown a higher luminosity either by photo- (~ 5.7 X) or by radio- excitation (~ 2.57 X). Their robustness against humidity has been demonstrated in a prolonged exposure to high humidity (75% RH) at an elevated temperature (60°C) for more than 200 hours. However, the emission wavelength of CsI(Tl) is centered at 540 nm which does not match well to the spectra response of conventional bi-alkali PMT tubes. Because of the greater overall light output of CsI(Tl) versus CsI(Na) (52,000 photons/MeV vs. 39,000 photons/MeV, respectively)[15] this issue is not as significant as it might appear.

After exposure to high humidity conditions, the surface of the Na activated CsI crystals develops a polycrystalline appearance. A "dead" layer or "inactive" domains can be detected by a 250 nm LED as the Na activators have been diffused out to the detector surface. In addition, the relative pulse height difference between the photopeak produced from an Am-241 source (60 keV) and the X-ray escape and the decay X-ray peak ($\sim$ 30 KeV) decreases. These features can be useful for screening of humidity damaged CsI crystals.

Microstructure study indicates that small crystallites are preferentially nucleated and developed at deeply scratched areas and the edges of the Na activated CsI crystals, where moisture condensation is most likely to occur. These areas expand as the exposure time in a high humidity environment increases. These small crystallites are nucleated and epitaxially recrystallized on the surface, suggesting that localized moisture condensation and recrystallization could be the culprit. The high solubility of NaI in water and localized condensation can exacerbate the out diffusion of Na in CsI(Na) detectors. Surface analysis by the ToF SIMS shows these recrystallized areas are rich in Na in comparison to its bulk crystal. The development of Na rich regions on crystal surface is indicative of lower Na concentration under these regions, leading to the development of "dead" layers or "inactive" regions in the bulk crystal. Therefore, the "inactive" region in the CsI(Na) detector is not an amorphous layer [4] nor a surface damaged layer [5]–[7], but is a region its activation concentration is below scintillation threshold due to the out diffusion of Na. These observations are consistent with scintillation degradation and highlight the importance of surface preparation for Na activated CsI detectors.

Acknowledgment

The authors would like to thank the following people for their contribution to this work: Clay Newton for humidity testing, Marlene Bencomo for pulse height measurement, Gary Zenker for SEM study, and Lam Banh for PMT fixture design and fabrication.

References

[1] J. Menefee, Y. Cho, and C. Swinehart, "Sodium activated cesium iodide as a gamma ray and charge particle detector," *IEEE Trans. Nucl. Sci.*, vol. NS-14, pp. 464–467, 1967.

[2] A. Synfeld-Kazuch, P. Sibczynski, M. Monszynski, A. V. Gektin, M. Grodzicka, J. Iwanowska, M. Szawlowski, T. Szczesniak, and L. Swiderski, "Performance of CsI(Na) scintillator in γ-ray spectrometry," in *Proc. IEEE Nuclear Science Symp. Conf. Rec.*, 2009, vol. N25-103, pp. 1474–1479.

[3] W. C. Kaiser, S. I. Baker, A. J. MacKay, and I. S. Sherman, "Response of NaI(Tl) to X-rays and low energy gamma rays," *IEEE Trans. Nucl. Sci.*, vol. NS-9, pp. 22–27, 1962.

[4] G. C. Kerrigan, B. H. O'Connor, and W. W. Thomas, "The deterioration in counting efficiency of a scintillation detector," *X-ray Spectrom.*, vol. 1, pp. 163–164, 1972.

[5] L. A. Andryushchenko, A. Yu. Boyarintsev, B. V. Grinyov, I. V. Kilimchuk, A. M. Kudin, V. A. Tarasov, and Y. T. Vydai, "Investigation of scintillation characteristics for CsI:Tl and NaI:Tl crystals under different surface treatment conditions," *Func. Mater.*, vol. 13, pp. 534–537, 2006.

[6] Y. T. Vydai, V. A. Tarasov, A. M. Kudin, L. A. Andryushchenko, A. A. Ananenko, I. V. Kilimchuk, A. Yu. Boyarintsev, and A. V. Klimov, "Stability of spectgrometric characteristics of CsI:Tl detectors depending on the surface treatment method," *Instrum. Exp. Tech.*, vol. 49, pp. 314–317, 2006.

[7] A. M. Kudin, L. A. Andryushchenko, V. Yu. Gres, A. V. Didenko, and T. A. Charkina, "How the surface-processing conditions affect the intrinsic luminescence of CsI crystals," *J. Opt. Technol*, vol. 77, pp. 300–302, 2010.

[8] K. V. Shahova, A. N. Panova, V. I. Goriletsky, Y. A. Prikhod'ko, V. P. Gavrylyuk, S. P. Korsunova, and N. N. Kosinov, "Luminescence and scintillation properties of Na-activated CsI-CsBr crystals," *Radiat. Meas.*, vol. 33, pp. 769–771, 2001.

[9] M. E. Keillor, M. W. Cooper, J. C. Hayes, and J. I. McIntyre, "Degradation of 81 keV $^{133}\mathrm{Xe}$ gamma-rays into the 31 keV X-ray peak in CsI scintillators," *J. Radioanal. Nucl. Chem.*, pp. 699–702, 2009.

[10] C. J. Crannell, R. J. Kurz, and W. Viehmann, "Characteristics of cesium iodide for use as a particle discriminator for high energy cosmic rays," Goddard Space Flight Center, Greenbelt, MD, USA, Tech. Rep. NASA TM X-70446, Aug. 1973.

[11] G. Kh. Rosenberg, Y. T. Vydai, G. V. Ptitsyn, and E. F. Chaikovskii, "Kinetics of the decay of a solid solution of Na at the surface of CsI crystals," *Bull. Acad. Sci. U.S.S.R.*, vol. 41, pp. 2365–2368, 1977.

[12] C. K. Ong, K. S. Song, R. Monnier, and A. M. Stoneham, "Electronic structure and luminescence of CsI:Na," *J. Phys. C, Solid State Phys.*, vol. 12, pp. 4641–4646, 1979.

[13] T. Sidler, J. P. Pellaux, A. Nouailhat, and M. A. Aegerter, "Study of V_k center in CsI crystal," *Solid State Commun.*, vol. 13, pp. 479–482, 1973.

[14] A. H. Kayal, Y. Mori, C. Jaccard, and I. Rossel, "Luminescence processes in CsI doped with Na^+ and K^+ ions," *Solid State Commun.*, vol. 35, pp. 457–460, 1980.

[15] P. Lecoq, A. Annenkow, A. Gektin, M. Korzhik, and C. Pedrini, *Inorgnaic Scintillators for Detection Systems*, A. Chao, T. Kondo, C. W. Fabjan, F. Ruggiero, and R.-D. Heuer, Eds. New York, NY, USA: Springer-Verlag, 2006, ch. 3, pp. 81–122.

[16] S. Masunaga, I. Morita, and M. Ishiguro, "Optical properties of CsI:Tl and CsBr:Tl," *J. Phys. Soc. Jpn.*, vol. 21, pp. 638–644, 1966.

[17] V. B. Gutan, L. M. Shamovskii, A. A. Dunina, and B. S. Gorobets, "Two types of luminescence centers in CsI:Tl," *Opt. Spectrosc.*, vol. 37, pp. 717–723, 1974.

[18] L. P. Smol'skaya and T. A. Kolesnikova, "Spectral features of CsI: Tl crystal phosphor," *Opt. Spectrosc.*, vol. 47, pp. 526–531, 1979.

[19] A. Fakuda, S. Makishima, T. Mabushi, and R. Ohaka, "Polarization of luminescence in KBr:Tl type crystals due to the Jahn-Teller effect," *J. Phys. Chem. Solids*, vol. 28, pp. 1763–1780, 1967.

[20] P. A. Rodnyi, *Physical Processes in Inorganic Scintillators*. Boca Raton, FL, USA: CRC Press, 1997.

[21] G. F. Knoll, *Radiation Detection and Measurements*, 3rd ed. New York, NY, USA: Wiley, 2000.

[22] P. G. Kotula, M. R. Keenan, and J. R. Michael, "Automated analysis of SEM X-ray spectral images: A powerful new microanalysis tool," *Microsc. Microanal.*, vol. 9, pp. 1–17, 2003.

[23] V. S. Smentkowski, J. A. Ohlhausen, P. G. Kotula, and M. R. Keenan, "Multivariate statistical analysis of time-of-flight secondary ion mass spectrometry images-looking beyond the obvious," *Appl. Surf. Sci.*, vol. 231-232, pp. 245–249, 2004.

[24] V. S. Smenkowski, M. R. Keenan, J. A. Ohlhausen, and P. G. Kotula, "Multivariate statistical analysis of concatenated time-of-flight secondary ion mass spectrometry spectral image. Complete description of the sample with one analysis," *Anal. Chem.*, vol. 77, pp. 1530–1536, 2005.

[25] V. I. Goriletsky, B. V. Grinyov, A. M. Panova, K. v. Shakhova, E. L. Vinograd, and S. P. Korsunov, "Kinetic and Scintillation Characteristics of CsI(Na) Crystals Grown under Melt Mixing," *Nucl. Instrum. Methods Phys. Res. B*, vol. 159, pp. 111–115, 1999.

[26] *Handbook of Chemistry and Physics*, 63rd ed. Boca Raton, FL, USA: CRC Press, 1984, pp. B92–B147.

[27] S. M. Klotsamn, I. P. Polikarpova, and A. N. Timofeev, "Self-diffusion of cesium-134 and diffusion of rubidium-86 in cesium iodide single crystals," *Phys. Stat. Sol. (b)*, vol. 49, pp. 423–430, 1972.